Journal of the Chinese Society of Mechanical Engineers, Vol.47, No.4, pp383~392 (2026)

Investigation of Ride Behavior of Rail Vehicle Using Analytical, Finite Element, Bond Graph and Experimental Method

Rakesh Chandmal Sharma*,**, Sunil Kumar Sharma***,
Sivasankara Raju Rallabandi****and Srihari Palli****

Keywords：**Bond graph technique, ISO-2631, ride comfort, Simulink block diagram.**

ABSTRACT

Vibrations in a railway coach are an important aspect that decides passengers' comfort level. These vibrations may be evaluated using several methods. The basis is to determine the inputs at the wheel-rail interface, then process them in terms of acceleration and assess the vehicle vibrations based on recommended comfort guidelines, i.e., the Sperling method, ISO-2631, etc. In the present work, a railway vehicle coach model is formulated using four approaches, i.e. analytical method (assigning it 37 degrees of freedom), BG-Simulink technique, Finite Element (Ansys) method and field testing. The ride comfort is determined under ISO-2631 comfort specifications using the rigid body (analytical) and flexible body (Ansys) models and then compared. The eigenfrequencies of the carbody are determined using analytical and Finite Element (Ansys) Methods. The eigenfrequencies determined from these methods compare well, justifying the model developed.

INTRODUCTION

The performance of the railway vehicle has improved significantly in the last two decades. The railway vehicle’s dynamic response evaluation involves deterministic and probabilistic analyses. Free vibration analyses are part of deterministic analysis used to extract the natural frequencies, and random response analysis is a probabilistic approach to obtain the dynamic vibrating parameters.

Researchers carried out studies to extract the natural frequencies using multi-body dynamics, computer-aided simulations using Finite Element Methods, and mathematical methods (Liu et al. 2022; Shao et al. 2023; Sharma, Palli, Sharma 2023). A hybrid metallic-composite (HMC) composed of railway axle is used to reduce the costly impact damage to the rail infrastructure (Johnson et al. 2022). The HMC railway axle comprises a full length, carbon fibre reinforced, epoxy matrix composite tube with secondary overwrapping for stiffness and EA1N grade steel collars creating the wheel seats and journal surfaces. A three-dimensional nonlinear wheel-rail contact model is presented to analyse the train-track-bridge coupled dynamics using he modal superposition method (Zeng, Liu, & Wang 2022). The eigenvalues were determined for the 5 degrees of freedom (DoF) bogie model and compared with the speed of the vehicle (Mazilu 2009). It is observed that the real part of the eigenvalues is detrimental to the bogie's stability at low rates. The critical speed is attained at 5 Hz, which is higher than the vehicle's yaw and lateral natural frequencies. These natural frequencies are compared with modal tests conducted with acceleration sensor equipment with a maximum error of 0.5 %. The measured wheel axle set accelerations on a corrugated track due to random unevenness are lower than generally expected from a 1 mm sweep disturbance for a BB series bogie used in EMU. Random track profiles in track alignment and gauge were fed as inputs to the 17 DoF Indian railway EMU coach lateral dynamic model in terms of Power Spectral Density (PSD) (Kumar, Kumar, Sujatha 2005). Assuming that the vehicle is travelling at 30 kmph, the lateral acceleration in g^2/Hz and displacement responses in terms of PSD have been obtained for the center of gravity (c.g.) of the vehicle.

The analytical formulation requires dealing with complex second-order partial differential equations. These difficulties can be overcome using

Paper Received March, 2025. Revised July, 2025. Accepted July, 2025. Author for Correspondence: Sunil Kumar Sharma.
**Professor, Mechanical Engineering Department, Graphic Era (Deemed to be University), Dehradun-248002, India email:rcsharmaiitr@gmail.com)*
***Adjunct Professor, Mechanical Engineering Department, Graphic Era Hill University, Dehradun, India*
***Assistant Professor, School of Technology, Gati Shakti Vishwavidyalaya, Vadodara-390004, India *email:sunilsharmaiitr@gmail.com*
*****Professor, Mechanical Engineering Department, Aditya Institute of Technology and Management, Tekkali, India email:srihari.palli@gmail.com*, sivaraju80@gmail.com

the bond graph technique, which eliminates the need to handle such lengthy equations. Once the model is formulated using bond graph (BG), the state-space first-order partial differential equations for generalized variables may be directly obtained, representing the system dynamic behavior. BG is an easier and more efficient approach to developing differential equations of the system without analyzing the physical field. BG technique may be investigated as a modeling tool for analyzing the dynamic response of road and railway vehicles (Kumar, Rastogi, Pathak 2018; Zeng and Dai 2021; Patel, Rastogi, & Borutzky 2023).

Researchers studied several software tools that process BG models of dynamic systems (Zhang et al 2022). It is established that Simulink, a MATLAB-based graphical programming platform for analyzing multi-domain dynamic systems, is a better choice. A few other software tools link explicitly with BG models, i.e. CAMP-G, TUTSIM, BONDLAB, through directly processing the flow lines (BONDLAB PH 2007; CAMP-G 2007; TUTSIM 2007).

The present paper presents a novel work in which a railway vehicle coach model is formulated using four different approaches, i.e. analytical method using Lagrangian method, BG-Simulink technique, Finite Element (Ansys) method and field testing. The ride behaviour of the vehicle is assessed using the abovementioned four methods for the model validation. The ride comfort is assessed under ISO criteria (ISO 1978, 1997) using rigid body (analytical) and flexible body (Ansys) models; and then compared. The eigenfrequencies of the carbody are determined using analytical and Finite Element (Ansys) Method. The eigenfrequencies determined from these methods compare well, justifying the model developed once again.

MATHEMATICAL MODELING (ANALYTICAL METHOD)

Vehicle Model

The railway vehicle model is formulated with Lagrangian method considering the carbody, bolster (2 in number), bogie frame (2 inre number) and wheel axle (4 in number) as the main rigid bodies, assigning 37 DoF overall to them (Figure 1).

The analytical model of vehicle and track is based on following assumptions.

- All mass assemblies are considered to be rigid bodies and vehicle structure is not deformable.
- Centre of gravity of all masses lie in central plane.
- Suspension elements are linear within the range of suspension travel.

Each considered nine rigid bodies are assigned vertical($z_1 \ldots z_9$), lateral ($y_1 \ldots y_9$) and roll ($\theta_1 \ldots \theta_9$) DoF. In addition, carbody and bogie frames are assigned pitch ($\varphi_1, \varphi_4, \varphi_5$) and yaw ($\psi_1, \psi_4, \psi_5$) DoF, wheel axles are assigned yaw DoF($\psi_6 \ldots \psi_9$). The system parameters and corresponding values have been mentioned in Table 1.

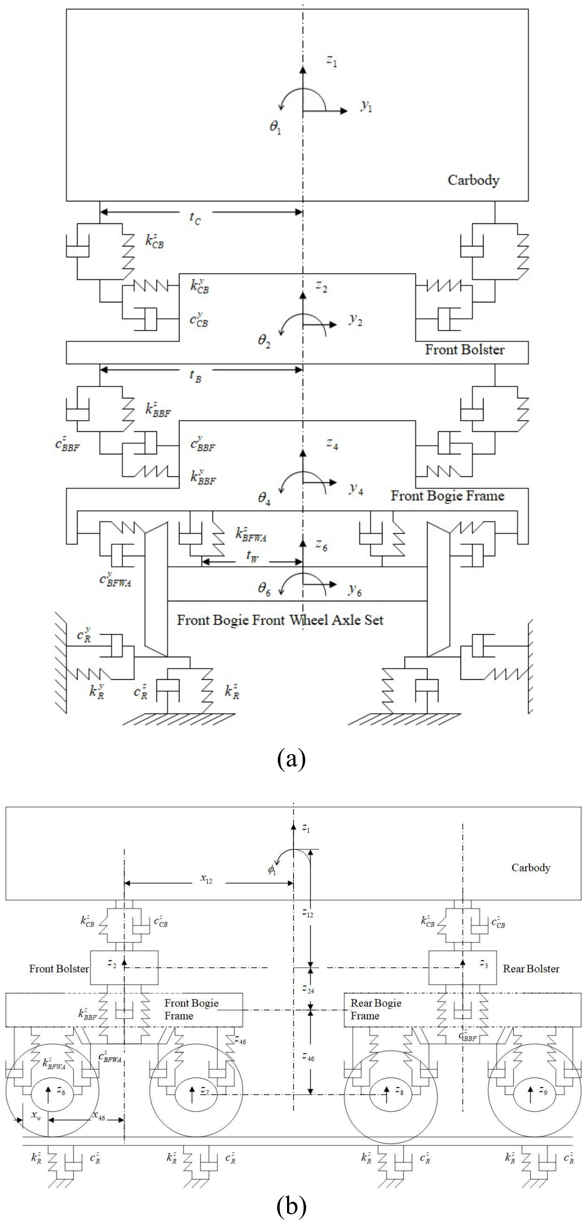

(a)

(b)

Figure 1. Rail-vehicle model (a) End View (b) Front view.

Track Model

The track may be divided into a super structure and a sub structure. The super structure includes rails, rail fastenings, pads, sleepers and ballast (i.e. soil). The sub grade or subsoil is the sub structure of a track. The track is assumed flexible vertically and laterally. Wheel is assumed in series with sleeper, soil and subsoil with linear suspension characteristics (Figure 2). For the soil and subsoil, per unit area vertical and lateral stiffness and damping are considered.

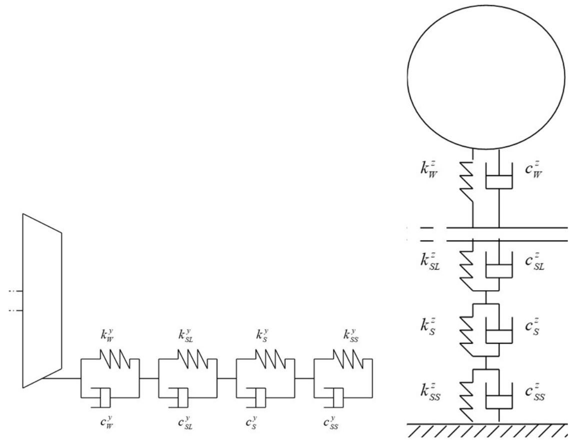

(a) (b)

Figure 2. Track model (a) End view (b) Front view

Table 1. System parameters and corresponding values.

Parameter	Value	Parameter	Value	Parameter	Value
M_C	33740 kg	$\boldsymbol{I_{ZWA}}$	1271 kg-m^2	f_{12}	1.5334 × 10^4 N
M_B	400 kg	t_C	0.8 m	$\boldsymbol{f_{22}}$	61.56 N m^2
M_{BF}	2600 kg	t_B	1.127m	k_{CB}^z	35 MN/m
M_{WA}	1600 kg	t_W	1.079 m	c_{CB}^z	0.035 MN-s/m
I_{XC}	56932 kg-m2	x_w	0.285	k_{CB}^y	17.5 MN/m
I_{YC}	1307220 kg-m2	δ	0.15 rad	c_{CB}^y	0.0175 MN-s/m
I_{ZC}	1309744 kg-m2	z_{12}	1.286 m	k_{BBF}^z	0.47 MN/m
I_{YB}	307 kg-m2	x_{12}	7.3915 m	c_{BBF}^z	0.0589 MN-s/m
I_{ZB}	336.4 kg-m2	z_{24}	0.1435	k_{BBF}^y	0.205 MN/m
I_{XBF}	1713 kg-m^2	z_{46}	0.209 m	$\boldsymbol{c_{BBF}^y}$	1 MN-s/m
I_{YBF}	3206 kg-m^2	x_{46}	1.448 m	$\boldsymbol{k_{BFWA}^z}$	0.26935 MN/m
I_{ZBF}	4763 kg-m^2	a	0.871 m	$\boldsymbol{c_{BFWA}^z}$	0.0206MN-s/m
I_{XWA}	1271 kg-m^2	r	0.457 m	$\boldsymbol{k_{BFWA}^y}$	11.5 MN/m
I_{YWA}	117 kg-m^2	f_{11}	7.5848 × 10^6 N	$\boldsymbol{c_{BFWA}^y}$	0.5 MN-s/m

Equations of Motions

For the present 37 DoF analytical model the equations of motion (EoM) are formulated using Lagrange's equations, which is generally expressed as:

$$\frac{d}{dt}\left[\frac{\partial L}{\partial \dot{q}_i}\right] - \frac{\partial L}{\partial q_i} + \frac{\partial E_P}{\partial q_i} + \frac{\partial E_D}{\partial \dot{q}_i} = Q_i \tag{1}$$

where L is Largrage's operator denoted as the difference of the kinetic energy and the gravitational potential energy function, E_P is spring strain energy function, E_D is the Rayliegh's dissipation energy function and Q_i is the generalized forces corresponding to q_i the generalized coordinates. The generalized forces of the system are evaluated using the principle of virtual work. The vehicle is assumed to be moving at uniform speed along straight track, therefore, DoF in longitudinal direction is not considered. The creep forces/moments and static forces at the wheel-rail interface due to the self-weight of the vehicle are determined using Kalker's linear theory of creepage (Kalker 1979) and quasistatic theory, respectively. Kalker's linear theory of rolling contact suggests that for small creepage, the area of spin is negligible, and its effect may be ignored. The adhesion zone, therefore, is considered to cover the entire area of contact.

The equations of motion of carbody for the present analytical model are expressed as follows:

The equation for lateral motion of car body

$$(M_C + 2M_1)\ddot{y}_1 + 2c_{CB}^y(2\dot{y}_1 - \dot{y}_2 - \dot{y}_3) + 4k_{CB}^y y_1 + M_1(\ddot{y}_2 + \ddot{y}_3) - 2k_{CB}^y(y_2 + y_3) + M_2(\ddot{y}_4 + \ddot{y}_5) + M_{WA}(\ddot{y}_p + \ddot{y}_q) + 2\mu_3(\dot{y}_p + \dot{y}_q) + 2(z_{12}M_1 + z_{24}M_2 + 2z_{46}M_{WA})\ddot{\theta}_1 + (z_{24}M_2 + 2z_{46}M_{WA})(\ddot{\theta}_2 + \ddot{\theta}_3) + 2z_{46}M_{WA}(\ddot{\theta}_4 + \ddot{\theta}_5) + \mu_1 f_{11}(\dot{\theta}_p + \dot{\theta}_q) + 2\mu_2(\dot{\psi}_p + \dot{\psi}_q) - 2f_{11}(\psi_p + \psi_q) = 0 \tag{2}$$

The equation for vertical motion of car body

$$(M_C + 2M_1)\ddot{z}_1 + c_{CB}^z\dot{z}_1 + 4k_{CB}^z z_1 + 2M_1(\ddot{z}_2 + \ddot{z}_3) - 2c_{CB}^z(\dot{z}_2 + \dot{z}_3) - 2k_{CB}^z(z_2 + z_3) + 2M_2(\ddot{z}_4 + \ddot{z}_5) + M_{WA}(\ddot{z}_p + \ddot{z}_q) + (M_C + 2M_1)g = 0 \tag{3}$$

The equation for roll motion of car body

$$[2z_{12}M_1 + 2z_{24}M_2 + 4z_{46}M_{WA}]\ddot{y}_1 + [z_{12}M_1 + z_{24}M_2 + 2z_{46}M_{WA})(\ddot{y}_2 + \ddot{y}_3) - 8F_Z - M_1 g(y_2 + y_3) + [p_4M_2 + 2z_{46}M_{WA}](\ddot{y}_4 + \ddot{y}_5) - 2(2y_4 + 2y_5 + y_p + y_q)F_Z + p_0M_{WA}(\ddot{y}_p + \ddot{y}_q) + \mu_1 f_{11}p_1(\dot{y}_p + \dot{y}_q) + [I_{XC} + 2(I_{X1} + z_{12}^2M_1 + (2z_{12} + z_{24}^2)M_2 + 2z_{46}(p_0 + p_4)M_{WA})]\ddot{\theta}_1 + 4c_{CB}^z t_C^2\dot{\theta}_1 - (8(F_Zp_1 - \mu_2\omega\delta a) - (8k_{CB}^z t_C^2 - 2M_1 g z_{12})\theta_1 + [I_{X1} + z_{24}p_4M_2 + 2p_0z_{46}M_{WA}](\ddot{\theta}_2 + \ddot{\theta}_3) - 2c_{CB}^z t_C^2(\dot{\theta}_2 + \dot{\theta}_3) - 4(F_Zp_2 - \mu_2\omega\delta a + k_{CB}^z t_C^2)(\theta_2 + \theta_3) - [I_{X2} + 2z_{46}p_0M_{WA}](\ddot{\theta}_4 + \ddot{\theta}_5) - 4(F_Zp_3 - \mu_2\omega\delta a)(\theta_4 + \theta_5) + I_{XWA}(\ddot{\theta}_p + \ddot{\theta}_q) + \mu_1 f_{11}p_1(\dot{\theta}_p + \dot{\theta}_q) - 2(F_Zr - \mu_2\omega\delta a)(\theta_p + \theta_q) + 2\mu_2p_1(\dot{\psi}_p + \dot{\psi}_q) - 2f_{11}p_1(\psi_p + \psi_q) = 0 \tag{4}$$

The equation for pitch motion of car body

$$-x_{12}M_1(\ddot{z}_2 - \ddot{z}_3 + \ddot{z}_4 - \ddot{z}_5) + 2c_{CB}^z x_{12}(\dot{z}_2 - \dot{z}_3) +$$

$$2k^z_{CB}x_{12}(z_2 - z_3) + M_{WA}(-x_1\ddot{z}_6 - x_2\ddot{z}_7 + x_2\ddot{z}_8 + x_1\ddot{z}_9) + (I_{YC} + 2I_{Y2} + 2z^2_{12}M_1 + 2x^2_{12}M_1 + 4z_{12}z_{24}M_2 + 2z^2_{24}M_2 + 4(z_{46}(p_0+p_4) + x^2_{46})M_{WA})\ddot{\varphi}_1 + (I_{Y2} + 2(p_3z_{46} + x^2_{46})M_{WA})(\ddot{\varphi}_4 + \ddot{\varphi}_5) - 8(F_Zp_0z_{12} - c^z_{BC}x^2_{12})\dot{\varphi}_1 - 2(F_Zp_3 + F_Zr + 2k^z_{BC}x^2_{12})\varphi_1 - 4F_Zp_3(\varphi_4 + \varphi_5) + 4F_Zr + 4k^z_{BC}x^2_{12})\varphi_1 - 2F_Za(2\psi_4 + 2\psi_5 + \psi_p + \psi_q) = 0 \quad (5)$$

The equation for yaw motion of car body

$$x_{12}M_1(\ddot{y}_2 - \ddot{y}_3) + 2c^y_{CB}x_{12}(\dot{y}_2 - \dot{y}_3) + 2k^y_{CB}x_{12}(y_2 - y_3) + x_{12}M_2(\ddot{y}_4 - \ddot{y}_5) + M_{WA}(x_1\ddot{y}_6 + x_2\ddot{y}_7 - x_2\ddot{y}_8 - x_1\ddot{y}_9) + 2(-\mu_2 + \mu_3x_1)\dot{y}_6 + 2(\mu_2 - \mu_3x_2)\dot{y}_7 + 2(-\mu_2 - \mu_3x_2)\dot{y}_8 + 2(-\mu_2 - \mu_3x_1)\dot{y}_9 + x_{12}(z_{24}M_2 + 2z_{46}M_{WA})(\ddot{\theta}_2 + \ddot{\theta}_3 + \ddot{\theta}_4 + \ddot{\theta}_5) - \mu_1(f_{12} + f_{11}x_1)\dot{\theta}_6 - \mu_1(f_{12} + f_{11}x_2)\dot{\theta}_7 - \mu_1(f_{12} + f_{11}x_2)\dot{\theta}_8 - \mu_1(f_{12} + f_{11}x_1)\dot{\theta}_9 + 4c^y_{CB}l^2_C\dot{\psi}_1 + 4k^y_{CB}x^2_{12}\psi_1 + (I_{ZC} + 2I_{Z1} + 2x^2_{12}M_1 + 4x^2_{46}M_{WA}\ddot{\psi}_1 + (I_{Z2} + 2x^2_{46}M_{WA})(\ddot{\psi}_4 + \ddot{\psi}_5) + I_{ZWA}(\ddot{\psi}_p + \ddot{\psi}_q) + 2(\mu_2x_1 + f_{22}/V)\dot{\psi}_6 - 2((f_{11}x_1 - f_{12} - M_{WA}g\delta a) + (f_{12}/r)\delta a)\psi_6 + 2(\mu_2x_2 + f_{22}/V)\dot{\psi}_7 - 2((f_{11}x_2 - f_{12} - M_{WA}g\delta a) + (f_{12}/r)\delta a)\psi_7 + 2(-\mu_2x_2 + f_{22}/V)\dot{\psi}_8 - 2((-f_{11}x_2 - f_{12} - M_{WA}g\delta a) + (f_{12}/r)\delta a)\psi_8 + 2(-\mu_2x_1 + f_{22}/V)\dot{\psi}_9 - 2((-f_{11}x_1 - f_{12} - M_{WA}g\delta a) + (f_{12}/r)\delta a)\psi_9 = 0 \quad (6)$$

The following substitutions have been provided to reduce the length of the Equations 2-6:

$M_B + M_{BF} + 2M_{WA} = M_1,\ M_{BF} + 2M_{WA} = M_2, I_{iB} + I_{iBF} + 2I_{iWA} = I_{i1}(\ i = X, Y, Z),\ I_{iBF} + 2I_{iWA} = I_{i2}\ \ (\ i = X, Y, Z),$

$$(z_{12} + z_{24} + z_{46}) = p_0, (z_{12} + z_{24} + z_{46} + r) = p_1, (z_{24} + z_{46} + r) = p_2, (z_{46} + r) = p_3, (z_{12} + z_{24}) = p_4, (z_{24} + z_{46}) = p_5, (x_{12} + x_{46}) = x_1\ , (x_{12} - x_{46}) = x_2$$

$$\left(\frac{2r}{V}\right) = \mu_1, \left(\frac{f_{12}}{V}\right) = \mu_2, \left(\frac{f_{11}}{V}\right) = \mu_3,$$

$(i_6 + i_7) = i_p(i = x, y, \theta, \psi), (i_8 + i_9) = i_q\ (i = x, y, \theta, \psi)$

EIGENVALUE ANALYSIS

Eigenvalue analysis (Analytical Method)

The eigenvalue analysis is performed to determine the stability of the present analytical model, transforming The eigenvalues of the matrix $[A]^{-1}[B]$ provide information for stability damped-undamped eigenfrequencies and decay rates of oscillations. The car body dynamic modes roll, pitch and bounce (vertical translation) are extracted under the unladen and laden conditions by lumping the masses. The tare mass of the coach considered in unladen condition is 52 tons. In contrast, in laden condition, an additional 4.68 tons is supposed to account for weighing 72 passengers with an average mass of 65 kg each. The bounce, pitch and roll mode frequencies of carbody are found to be 0.66 Hz, 0.7 Hz and 3.20 Hz in unladen condition, whereas in laden condition those values are 0.6 Hz, 0.66 Hz and 3.02 Hz respectively.

The state space first-order differential EoM is expressed as follows:

$$[A](\dot{X}) = [B](X) \quad (8)$$

$(\dot{X}) = [\dot{X}_1, \dot{X}_2, \dot{X}_3, , \dots \dots \dots . \dot{X}_{73}\ ]$ and

$is\ [X_1, X_2, X_3 \dots \dots X_{74}] \quad (9)$

$$(\dot{X}) = [A]^{-1}[B](X) \quad (10)$$

The eigenvalues of the matrix $[A]^{-1}[B]$ provide information for stability damped-undamped eigenfrequencies and decay rates of oscillations. The car body dynamic modes roll, pitch and bounce (vertical translation) are extracted under the unladen and laden conditions by lumping the masses. The tare mass of the coach considered in unladen condition is 52 tons. In contrast, in laden condition, an additional 4.68 tons is supposed to account for weighing 72 passengers with an average mass of 65 kg each. The bounce, pitch and roll mode frequencies of carbody are found to be 0.66 Hz, 0.7 Hz and 3.20 Hz in unladen condition, whereas in laden condition those values are 0.6 Hz, 0.66 Hz and 3.02 Hz respectively.

Eigenvalue analysis (Finite Element method)

Following are the assumptions with the Finite Element modeling.

- Berths, electric equipment, and other aesthetically pleasing coach interior characteristics are not taken into consideration.
- Shells are modelled as thin surfaces with a 2 mm thickness to represent the interior and external walls around the shell's structural parts, such as solebars, cant rails, stanchions, and spaces in between window panels. This approach treats shells as thin-walled hollow girders.
- The coach's over-body length is taken into account only; the over-buffer length is omitted.
- The primary and secondary suspension elements are linear.
- Since the car's shell makes up the majority of its body, the hollow-shelled construction is thought to be devoid of any inside components.
- To account for the stiffness between the body bolsters and the car body, constraint equations with line elements are used.

These modal frequencies of the railway car body are further simulated using finite element analysis in ANSYS. The bounce, pitch and roll mode shapes of the railway coach subjected to laden and unladen conditions are depicted below (Figures 3, 4, 5, 6, 7 and

8). The extracted dynamic modes in ANSYS, indicate that the front and rear ends of the coach are subjected to higher displacements in bounce and pitch modes, whereas the top portion of the coach is subjected to higher displacements in roll mode. The natural frequencies of the coach obtained in Finite Element Method are compared with that of the modes of the developed mathematical model and listed in Table 2.

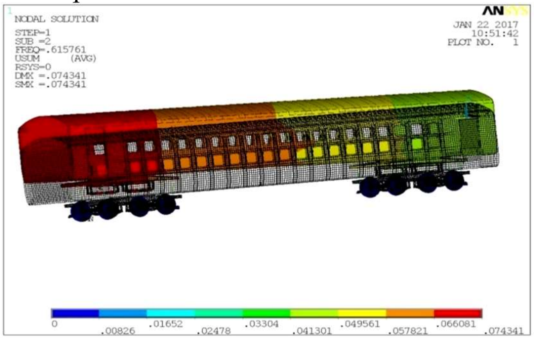

Figure 3. Bounce Mode of ICF Coach (Unladen) at 0.616 Hz.

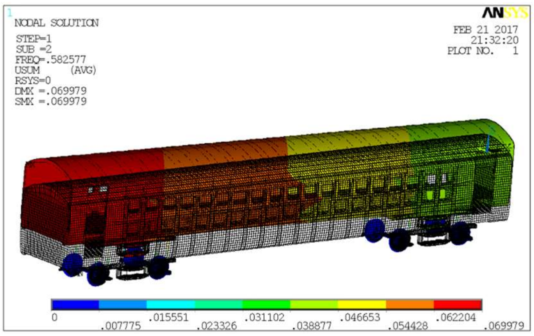

Figure 4. Bounce Mode of ICF Coach (laden) at 0.583 Hz.

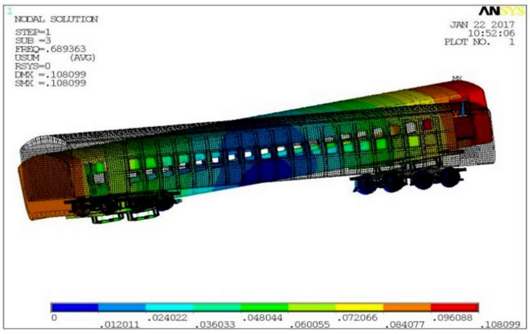

Figure 5. Pitch Mode of ICF Coach (Unladen) at 0.689 Hz.

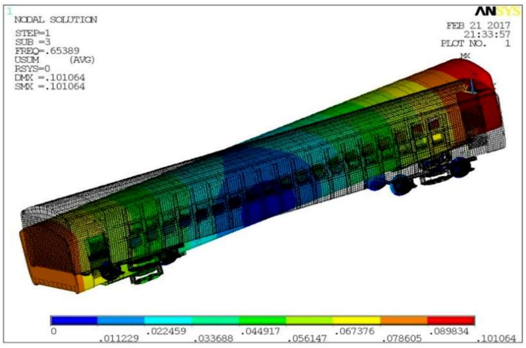

Figure 6. Pitch Mode of ICF Coach (laden) at 0.654 Hz.

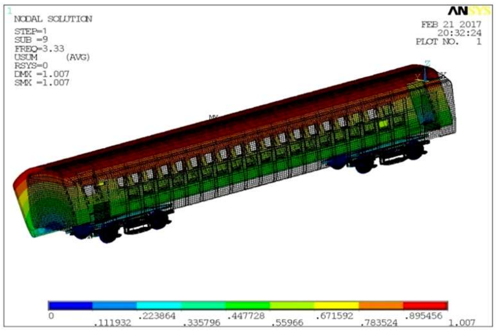

Figure 7. Roll Mode of ICF Coach (Unladen) at 3.33 Hz.

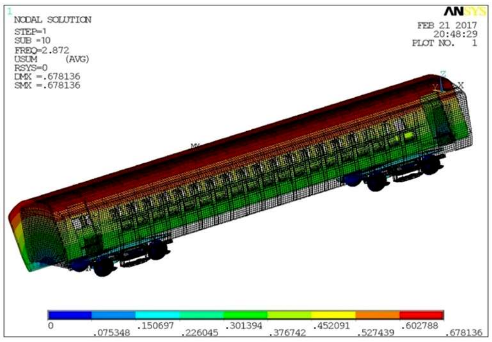

Figure 8. Roll Mode of ICF Coach (laden) at 2.872 Hz.

Table 2. Natural Frequencies of Coach Model with Finite Element and Analytical Methods.

Mode	Ansys (Hz)	Mathematical Model (Hz)	Percentage Difference
Unladen Coach			
Bounce	0.616	0.66	6.67%
Pitch	0.689	0.70	1.57%
Roll	3.33	3.2	4.06%
Laden Coach			
Bounce	0.583	0.6	2.83%
Pitch	0.654	0.66	0.90%
Roll	2.872	3.02	4.90%

ANALYSIS OF RIDE (ANALYTICAL METHOD)

Description of random input

The track profile of a wavelength ranging between 0.1 to 100 m is of prime interest to track designers. Since track profiles are featured as probabilistic, they are more suitable to be represented by statistical techniques. The track parameters are assessed for a distance of 0.404 m by using Track Recording Car (TRC) by Research Designs Standards Organisation (RDSO), Lucknow (India).

The sample output provided by TRC is listed in Table 3. In Table 3 UNL, UNR, XL, ALL, ALR, G, CAV, CAL, TW, V and GF stands for Unevenness (left rail), Unevenness (right rail), Cross-level, Alignment (left), Alignment (right), Gauge, Coach Acceleration Vertical, Coach Acceleration Lateral, Twist, Speed and Ground Feature respectively.

Table 3. Rail profile parameters provided by TRC.

TGMS-10 VERSION 1.40, RAW DATA PROFILES

UNL ×4	UNR ×4	XL× 4	ALL ×4	ALR ×4	G× 4	CAV	CAL	TW× 4	V	GF
37	-11	-43	7	6	13	36	33	-33	20906	0
35	-10	-41	8	8	13	40	-40	-33	19805	0
34	-7	-42	9	8	15	30	-42	-32	19409	0
36	-6	-39	9	7	14	32	-30	-27	19594	0
35	-5	-38	9	7	15	32	-20	-27	20433	0

The track irregularities at a future instant cannot be predicted and, therefore are classified as random.

The TRC sample output is further processed using Fast Fourier Transformation (FFT) to express the auto and cross PSD's of track undulations expressed in the following form.

$$S(\Omega) = C_{SP}(\Omega)^{-N} \tag{11}$$

C_{SP} is a constant, and N is the rate of amplitude reduction relative to frequency.

For the matrix $[S_r(\Omega)]_{8\times8}$ of track input, the auto and cross PSD elements and corresponding values of C_{SP} and N are given in Table 4.

Table 4. The values of C_{SP} and *N*.

S.N	Elements of $S^{z,y}(\Omega)]_{8\times8}$	C_{SP}	N
1	$S_{11}^z(\Omega), S_{22}^z(\Omega),\ldots S_{88}^z(\Omega)$	0.0958	-2.1382
2	$S_{12}^z(\Omega)$, $S_{34}^z(\Omega)$, $S_{56}^z(\Omega)$, $S_{78}^z(\Omega)$	0.0257	-2.3945
3	$S_{11}^y(\Omega)$,$S_{22}^y(\Omega)$,….$S_{88}^y(\Omega)$	0.0554	-2.2686
4	$S_{12}^y(\Omega)$, $S_{34}^y(\Omega)$, $S_{56}^y(\Omega)$, $S_{78}^y(\Omega)$	0.0287	-2.3082

The other elements may be described through a time lag among the contact points e.g. $S_{14}^z(\Omega) = 0.0257(\Omega)^{-2.3945}e^{-i\omega T}$. The functions $S_{14}^z(\Omega)$ and $S_{41}^z(\Omega)$ are identical; however, the signs of their imaginary parts are different.

PSD and Root Mean Square (RMS) Acceleration Response

The EoM the analytical model in the general form, is expressed as:

$$([\boldsymbol{M}](-\boldsymbol{\omega}^2) + [\boldsymbol{C}](\boldsymbol{i\omega}) + [\boldsymbol{K}])\boldsymbol{y_i e^{i\omega t}} = [\boldsymbol{F_r(\omega)}]\boldsymbol{q_r e^{i\omega t}} \tag{12}$$

Meanwhile, [M], [K] and [C] are the standard notations and $[\boldsymbol{F_r(\omega)}]$ is the force matrix of wheel-rail interactions.

The equation (12) may be further expressed as:

$$[\boldsymbol{D}]\boldsymbol{H_r(\omega)} = \boldsymbol{F_r(\omega)} \qquad \boldsymbol{where\ H_r(\omega) = y_i/q_r} \tag{13}$$

PSD or mean square acceleration response *(MSAR)* of carbody c.g. is expressed as:

$$\boldsymbol{MSAR} = (\boldsymbol{2\pi f})^4[\boldsymbol{H_r(\omega)}][\boldsymbol{S_r(\omega)}][\boldsymbol{H_r(\omega)}]^{\boldsymbol{T}} \tag{14}$$

RMS acceleration response (RMSAR) of carbody c.g. is expressed as:

$$\boldsymbol{RMSAR} = \boldsymbol{sqrt}\left[\left(\boldsymbol{2\pi}\right)^4 \int_{\boldsymbol{0.89fc}}^{\boldsymbol{1.12fc}} \left[\boldsymbol{S(f)}\right](\boldsymbol{f})^4\boldsymbol{df}\right] \tag{15}$$

BOND GRAPH MODELING

The fundamental property of a system is energy. It exchanges between two sources, stored in system elements on a transient basis or partly discharged in friction or heat, and then reaches "*sinks*" or "*loads*" to serve the objectives. The power is a scalar term and requires no path. However, power is difficult to evaluate straightway and is determined using two transient variables known as '*flow*' and '*effort'*. These variables have different values based on the type of system, e.g. for a mechanism, flow is indicated by 'velocity' and effort by 'force'. On each *Bond*, one variable is the origin, and the other is the outcome. An arrowhead represents the relationship. The effort and flow are presented at the two ends in a *Bond*.

The BG sub-model of the vehicle components considered for the analytical model is shown in Figures 9, 10, 11 and 12, respectively. In the present work, each component is formulated independently. Furthermore, all components are integrated and formulated into a complete single model of the system, analyzed with the Simulink block diagram approach. The modeling assumptions with the present BG method are similar to that used for the analytical method. The linear and angular velocities of the rigid bodies of the railway vehicle is represented by 1-junction, and these velocities are linked through longitudinal and lateral distances between the mass centre of these bodies via Transformer port 'TF'. The spring stiffness and the damping coefficient between the rigid bodies are represented by Compliance port 'C' and Resistance port 'R', respectively. The mass of the rigid body is represented by Inertia port 'I', and the weight of the rigid body is considered as the negative source of effort 'SE', which supplies the traction effort.

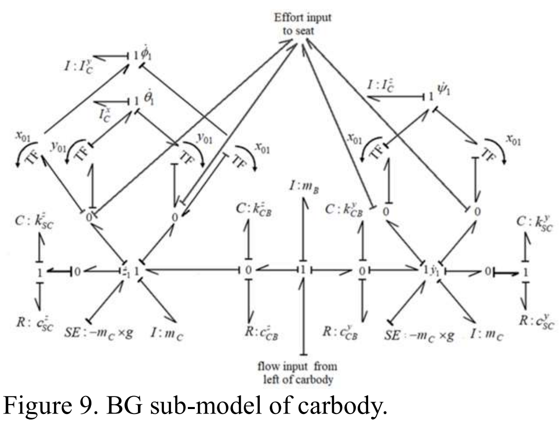

Figure 9. BG sub-model of carbody.

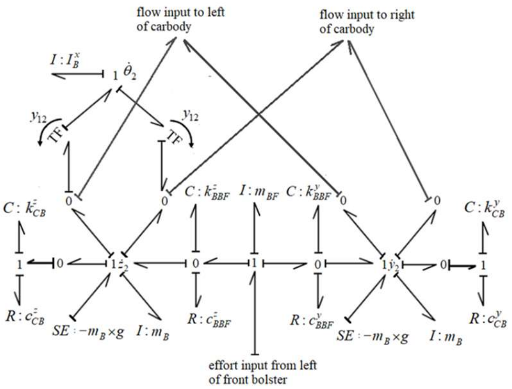

Figure 10. BG sub-model of bolster.

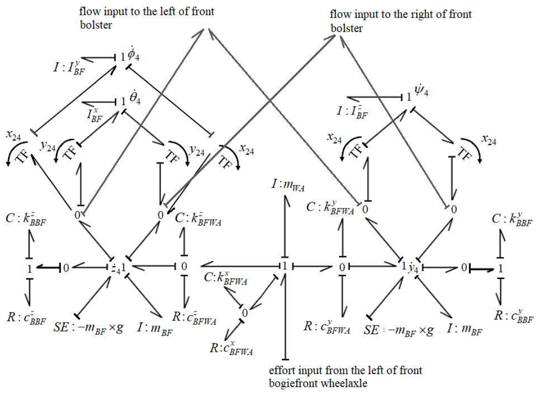

Figure 11. BG sub model of bogie frame.

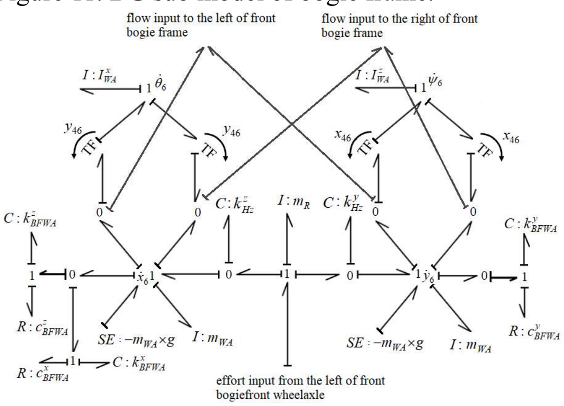

Figure 12. BG sub-model of wheelaxle.

DESCRIPTION OF EXPERIMENTAL TESTING

Simulated vertical and lateral PSD acceleration evaluated at the carbody c.g. is compared with field test carried out by Research Designs Standards Organisation, Lucknow, INDIA. The rail vehicle travelled at a constant speed of 100 km/hr on a straight track.

The field test is conducted in two stages. The first stage measures the accelerations for 2 km tangent run-down track. In the next stage, this measurement is justified for a distance of nearly 25 km. A strain gauge accelerometer (Range: ±1 g and ±2 g; Excitation: 5V AC/DC; Sensitivity: 360 mV/V/g; Damping: silicon fluid) is used for acceleration measurements. For the evaluation of ride quality, ability of vehicle suspension (to keep the motion within limits of human comfort and/or in limits to ensure minimum lading damage) is assessed, and the sensor is kept at the bogie level, as shown in Figure 13. The acceleration values obtained at this place are relatively higher. For the evaluation of ride comfort, the vehicle is examined based on the effect of mechanical vibrations on the occupant. For this purpose, the sensor is kept on the floor level of the central bogie pivot, as shown in Figure 14. It is considered that at this place, the vibrations or accelerations measured are the same as those experienced by the occupant during his travel. The acceleration data is sampled in the time domain using National Instruments cards (sampling rate, 100 samples/s; resolution, 12 bit) with LabView software, and this data is transformed into the frequency domain using FFT.

Figure 13. Measurement of acceleration through field test (sensor kept at bogie level).

Figure 14. Measurement of acceleration through field test (sensor kept at floor level of central bogie pivot).

RESULTS AND DISCUSSIONS

PSD Acceleration Response (Validation of model)

From analytical, Finite Element, Bond graph method and experimental measurements, vertical PSD acceleration and lateral PSD acceleration curves have been shown in Figures 15 and 16, respectively. The methods mentioned above used for the evaluation of PSD accelerations in the present work have their limitations; therefore, slight discrepancies in the results are possible. These discrepancies are due to simplified assumptions associated with each method and some other practical difficulties. The analytical method evaluates the acceleration with reference to c.g. of the carbody. In contrast, with field measurement, the sensor is kept at the floor level of bogie pivot, which does not exactly represent the c.g. of the carbody. The suspension elements, creep forces, wheel-track interaction, wind drag forces, etc are quite difficult to model very accurately with the considered methods. All these facts lead to slight discrepancies in the results. However, Figures 15 and 16 suggest that results obtained from analysis and field test were in acceptable compliance; therefore, the modeling using different methods is reasonably authenticated.

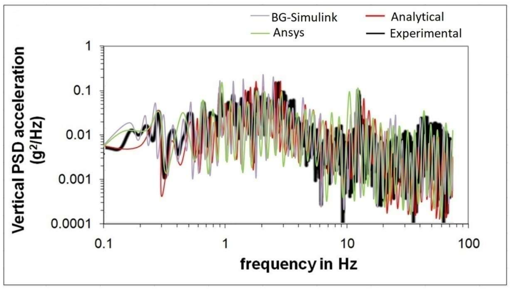

Figure 15. Vertical PSD acceleration at carbody mass centre (simulation and experimental).

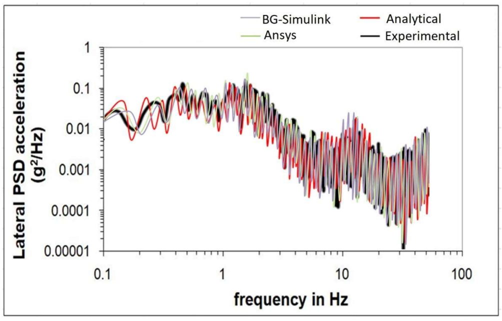

Figure 16. Lateral PSD acceleration at carbody mass centre (simulation and experimental).

Ride comfort evaluation

Several standards have been proposed to assess human exposure to whole-body vibration and repeated shock. It is challenging to determine the tolerance of human vibration to vehicle ride vibration despite extensive efforts done by researchers. Thus, there is no concurrence on a criterion accepted worldwide for evaluating ride comfort. However, the International Standard Organization (ISO) regulations are one of the most unanimously accepted criteria for ride comfort evaluations. In the present work, the frequency-weighted RMS values are evaluated for ride comfort criterion based on multi-axis whole-body vibrations (ISO 1997). Figures 17 and 18 show the weighted vertical and lateral RMSAR at the carbody mass centre in one-third octave bands obtained using rigid body (analytical) and flexible body (Ansys) models.

The ride comfort in vertical and lateral directions is determined for the duration of 1, 2.5, 4 and 8 hours for a speed of 100 km/hr.

With the rigid body (analytical) model, the weighted vertical RMS acceleration lies within 1 hrs comfort limit and exceeds the 2.5 hours ISO comfort limit (ISO 1978) for 5.05 Hz to 8.05 Hz. It exceeds 4 hours of ISO comfort limits of 4.3 Hz to 8.95 Hz and crosses 8 hours of ISO comfort limit for 3.1 Hz to 17.9 Hz (Figure 17). The weighted lateral RMS acceleration (Figure 18), lies within the comfort limit apart from 3.25 to 3.65 Hz for the duration from 1 hour to 8 hours at the considered speed.

With the flexible body (Ansys) model, the weighted vertical RMS acceleration lies within 1 hour comfort limit. It exceeds the 2.5 hours ISO comfort limit for 4.3 Hz to 6.15 Hz and from 6.45 to 6.8 Hz. It exceeds 4 hours ISO comfort limits for 4.1 Hz to 9 Hz and from 10.5 to 11.3 Hz and crosses 8 hours ISO comfort limit for 3.9 Hz to 14 Hz (Figure 17). The weighted lateral RMS acceleration curve (Figure 18), with the flexible body (Ansys) model, is quite similar to that of the rigid body (analytical) model; however, peak lateral acceleration value is observed at slightly higher frequency and acceleration values crosses the 1 hour to 8 hours comfort boundaries for a broader frequency range.

RMSAR is the measure of vibration evaluation as per ISO criteria (ISO 1997). As per its guidelines, the value of overall weighted acceleration in vertical directions a_{Wz} is

$$a_{Wz} = [\sum(W_k a_{iz})^2]^{1/2}. \qquad (16)$$

and the value of overall weighted acceleration in lateral directions a_{Wy} is

$$a_{Wy} = [\sum(W_d a_{iy})^2]^{1/2}. \qquad (17)$$

The vibration total value of weighted RMS acceleration, which is the ride index of the vehicle as per annexure ISO 2631-1 (ISO 1997), is expressed as:

$$a_v = [k_y^2 a_{Wy}^2 + k_z^2 a_{Wz}^2]^{1/2} \qquad (18)$$

The overall weighted RMS acceleration in vertical and lateral directions from the present analytical method is evaluated as 1.04 m/s^2 and 0.42 m/s^2, respectively. These overall weighted RMS vertical and lateral acceleration values with the flexible body (Ansys) model are obtained as 1.12 m/s^2 and 0.53 m/s^2, respectively. The ride index of the vehicle with rigid body (analytical) and flexible body (Ansys) models are determined as 1.19 m/s^2 and 1.34 m/s^2, respectively; both the values lie in the level of 'uncomfortable' as per ISO 2631-1 specifications.

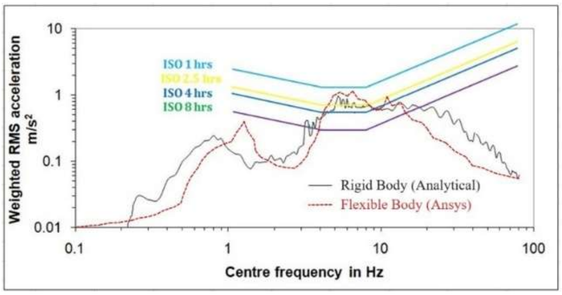

Figure 17. Weighted vertical RMS acceleration at carbody c.g. at 100 km/hr for rigid body (analytical) and flexible body (Ansys) models.

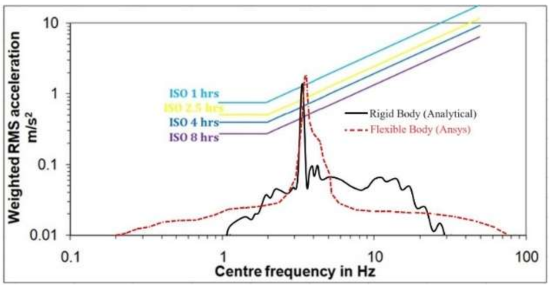

Figure 18. Weighted lateral RMS acceleration at carbody c.g. at 100 km/hr for rigid body (analytical) and flexible body (Ansys) models.

CONCLUSIONS

In the present work, the ride and eignevalue analysis of Indian railway vehicle is performed using four methods, i.e. analytical, Finite Element, Bond Graph and experimental. The following key findings have been obtained from the present analysis.

- The eigenvalues of the carbody/coach, evaluated using both the analytical and finite element methods, are in reasonable agreement.
- The PSD acceleration of the vehicle carbody is evaluated using analytical, Finite Element, Bond Graph and experimental methods, and it is found in good agreement, thereby justifying the formulated model.
- The weighted vertical and lateral RMSAR are evaluated using an analytical and Finite Element method based on ISO and ISO 2631 comfort specifications for 1, 2.5, 4, and 8 hours comfort boundaries.
- The ride index of the vehicle with rigid body (analytical) and flexible body (Ansys) models are determined as 1.19 m/s^2 and 1.34 m/s^{2,} respectively; both values lie in the level of 'uncomfortable' as per ISO 2631-1 specifications.
- The natural frequencies of different segments lie within 15 Hz, it can be concluded that the Indian Railway Integral Coach Factory coach is not justifying the 8-hour travel requirements. The lateral RMS acceleration exceeds the comfort limits for a small frequency range of nearly 3.5 Hz; therefore, it is not critical relative to vertical RMS acceleration.

The methods used for the evaluation of ride behavior in the present work may be extended in the assessment of other performance indices, i.e. stability or curving behavior. A biodynamic human model may also be integrated with vehicle seats, and the ride comfort analysis may be extended to various segments of the human subject.

Nomenclature:

a *Half the wheel gauge*

$c_{ij}^{z,y}$ Vertical and lateral damping coefficient respectively among the components (*i≠ j = C, B,BF, and WA, C= Carbody, B= Bolster,, BF= Bogie Frame, WA=Wheel Axle)* (In Figure 1b c_{CB}^{z} is ½ part, c_{BBF}^{z} is ½ part, c_{BFWA}^{z} is ¼ part) (MN-s/m)

$c_{R}^{z,y}$ Vertical and lateral track damping coefficient respectively (MN-sec/m)

f_i Creep coefficients (i=11, 22 *and* 12*: notations as per international standards)*

F_Z Static force at the wheel-rail contact point due to the self-weight of the vehicle

$I_{X,Y,Zi}$ Roll, pitch, and yaw mass moment of inertia (MI) respectively of components (*i= C, B, BF and WA)* (kg-m^2)

k_{ij}^{z} Vertical stiffness among components (*i≠ j = C, B, BF, and WA)* (In Figure 1b k_{CB}^{z} is ½ part, k_{BBF}^{z} is ¼ part, k_{BFWA}^{z} is ¼ part) (MN/m)

$k_{R}^{z,y}$ Vertical and lateral track stiffness, respectively (MN/m)

$k_{i}^{z,y}$ Vertical and lateral stiffness (*i= W (wheel), SL (sleeper), S (soil), SS* (sub soil) respectively (MN/m)

$k_{y,z}$ Multiply factors to RMS acceleration as specified in annexure ISO 2631-1 (ISO 1997)

M_i Vehicle component mass (*i = C, B, BF and WA*) (kg)

r Radius of the wheel of the wheel axle set corresponding to the track center line

t_i Lateral distance between vehicle components as shown in Figure 1b. (*i= C, B, W)* (m)

V Vehicle linear velocity (m/s)

$W_{k,d}$ Principal weighting factors as specified in annexure ISO 2631-1 (ISO 1997)

x_{ij} The horizontal distance between components c.g. (*i≠ j* =1, 2, 4, 6 *i.e.* 1 *for Carbody,* 2 *for Bolster,* 4 *for Bogie Frame, and* 6 *for Wheel Axle)* (m)

z_{ij} Vertical distance among components c.g. (*i≠ j* = 1, 2, 4, 6) (m)

δ Conicity wheel of the wheel axle set corresponding to the track center line

ω Wheel angular velocity (rad/s)

10.29979/JCSME.202608_47(4).0008

Conflict of interest

The authors declare that they have no conflicts.

References

BONDLAB. PH. Department Silicon Facility (DSF). http://ssd-rd.web.cern.ch/ssd-rd/bondlab/default.htm, (September 2007).

CAMP-G. “Computer Aided Modelling, Design and Simulation”. http://www.bondgraph.com, (September 2007).

International Organization for Standardization (ISO), ISO 2631:1978. 1978. Guide for the Evaluation of Human Exposure to Whole Body Vibrations, ISO, Geneva. (accessed 30 April 2016). Avasilable at: http://www.iso.org/iso/rss.xml?csnumber=7608&rss=detail

ISO (International Organization for Standardization). Mechanical Vibration and Shock Evaluation of Human Exposure to Whole Body Vibrations-Part 1: General requirements, Geneva, Switzerland. ISO 2631-1:1997. Geneva: ISO/TC 108/SC 4 (1997).

Johnson, M.S., Evans, R., Mistry, P.J., Li, S., Bruni, S., Bernasconi, A. and Cervello, S. "Structural Analysis for the Design of a Lightweight Composite Railway Axle." Composite Structures, Vol. 290, pp. 115544 (2022).

Kalker, J.J. “Survey of Wheel-Rail Rolling Contact Theory.” Vehicle System Dynamics Vol. 8, No. 4, pp. 317–358 (1979).

Kumar, H., B.S. Kumar and C. Sujatha. “Lateral Dynamic Analysis of a Typical Indian Rail-Road Vehicle”. Proceedings of 12th National Conference on Machines and Mechanisms (NaCoMM-2005), IIT Guwahati, December 16-17, pp. 208-214 (2005).

Kumar, V., V. Rastogi and P.M. Pathak. “Modelling and Evaluation of the Hunting Behaviour of a High-Speed Railway Vehicle on Curved Track”. Proceedings of the Institution of Mechanical Engineers, Part F: Journal of Rail and Rapid Transit Vol. 233, pp. 1-17 (2018).

Liu, L. Z. Zuo, J. D. Yau, and S. Urushadze. “A Simplified Method to Assess Vehicle–Bridge Interaction for Train-Induced Vibration of Light-Weight Railway Bridges.” Journal of the Chinese Institute of Engineers Vol. 45, No. 8, pp. 651-660 (2022).

Mazilu, T. “An Analysis of Bogie Hunting Stability”. U.P.B. Science Bulletin Sr D, Vol. 71, No. 63-78.

Patel, Y., Rastogi, V., & Borutzky, W. “Simulation Study on the Influence of Wheel Irregularity on the Vertical Dynamics of Wheel–Rail Interaction for High-Speed Railway Track using Bond Graph”. Simulation, Vo. 99, No. 6, pp. 643-656 (2023).

Shao, S., K. Zhang, Y. Yao, and Y. Zhang. “Investigation of the Sealing Performance of the Gearbox Sealing System of High-Speed Trains.” Journal of the Chinese Institute of Engineers Vol. 46, No. 1, pp. 63-73 (2023).

Sharma, R.C., S. Palli and S.K. Sharma. “Ride Analysis of Railway Vehicle considering Rigidity and Flexibility of the Carbody.” Journal of the Chinese Institute of Engineers Vol. 46, No. 4, pp. 355–366 (2023).

TUTSIM. Technical University of Twente SIMulation, University of Twente (2007). http://www.20sim.com/tutsim.html, (September 2007).

Zhang, Y., Li, L., Liu, W., Li, L., Gao, Y.E., Cai, W., & Sutherland, J.W. “Dynamics Analysis and Energy Consumption Modelling based on Bond Graph: Taking the spindle system as an example.” Journal of Manufacturing Systems, Vol. 62, pp. 539-549 (2022).

Zeng, J. and Dai, H. “The Dynamic Simulation of Vehicle–Bridge Interactions Using Bond Graph Technique.” In The Dynamics of Vehicles on Roads and on Tracks, pp. 591-602 (2021).

Zeng, Z.P., Liu, F.S., & Wang, W.D. “Three-Dimensional Train–Track–Bridge Coupled Dynamics Model based on the Explicit Finite Element Method.” Soil Dynamics and Earthquake Engineering, Vol. 153, pp. 107066 (2022).